Journal of Hazardous Materials 217–218 (2012) 315–322

Contents lists available at SciVerse ScienceDirect

Journal of Hazardous Materials

journal homepage: www.elsevier.com/locate/jhazmat

Differential pulse voltammetric determination of methyl parathion based on multiwalled carbon nanotubes–poly(acrylamide) nanocomposite film modified electrode

Yanbo Zeng[a,b], Dajun Yu[a], Yanyan Yu[a], Tianshu Zhou[c], Guoyue Shi[a,*]

[a] Department of Chemistry and Shanghai Key Laboratory of Green Chemistry and Chemical Process, East China Normal University, 3663 Zhongshan Road(N), Shanghai, 200062, PR China
[b] College of Biological, Chemical Sciences and Engineering, Jiaxing University, Jiaxing 314001, PR China
[c] Department of Environmental Science, East China Normal University, 3663 Zhongshan Road(N), Shanghai, 200062, PR China

ARTICLE INFO

Article history:
Received 21 December 2011
Received in revised form 16 February 2012
Accepted 10 March 2012
Available online 20 March 2012

Keywords:
Multiwalled carbon nanotubes–poly(acrylamide) nanocomposite
Organophosphorus pesticides
Methyl parathion
Differential pulse voltammetry
Electrochemical sensor
Environmental water samples

ABSTRACT

A sensitive electrochemical differential pulse voltammetry method was developed for detecting methyl parathion based on multiwalled carbon nanotubes–poly(acrylamide) (MWCNTs–PAAM) nanocomposite film modified glassy carbon electrode. The novel MWCNTs–PAAM nanocomposite, containing high content of amide groups, was synthesized by PAAM polymerizing at the vinyl group functionalized MWCNTs surface using free radical polymerization. The MWCNTs–PAAM nanocomposite was characterized by Fourier transform infrared spectroscopy, thermal gravimetric analysis and scanning electron microscopy. Electrochemical behavior and interference studies of MWCNTs–PAAM/GCE for methyl parathion were investigated. The experimental results demonstrated that the MWCNTs–PAAM/GCE exhibited a high adsorption and strong affinity toward methyl parathion compared with some metal ions and nitroaromatic compounds, which exist in environmental samples. The adsorbed amount of methyl parathion on the MWCNTs–PAAM/GCE approached the equilibrium value upon 5 min adsorption time. A linear calibration curve for methyl parathion was obtained in the concentration range from 5.0×10^{-9} to 1.0×10^{-5} mol L^{-1}, with a detection limit of 2.0×10^{-9} mol L^{-1}. The MWCNTs–PAAM/GCE was proved to be a suitable sensing tool for the fast, sensitive and selective determination of methyl parathion in environmental water samples.

1. Introduction

Organophosphorus (OP) pesticides have been widely used to protect agricultural crop against damaging caused by insect pests. During and after their application in agriculture, OP pesticides are transported by wind or water to environment as only a part of the applied amounts is bioactive [1,2]. This transport results in hazardous concentrations of pesticides and their metabolites in the surface water and soils, owing to their low solubility and bioaccumulation properties [3]. Thus, extensive usage of OP compounds with high toxicity has raised serious public concern regarding a great harm to humans and the environment [4]. Their toxicity depends on inhibiting the activity of enzymes controlling the functions of the nervous system, mainly acetylcholinesterase, which results in accumulation of acetylcholine at nerve endings. Excess acetylcholine at synaptic junctions in neurons causes fasciculation and disrupts normal neural transmission, which leads to a state of hyperarousal, and paralysis of the muscles and the main respiratory center [5]. Therefore, for the sake of human health and environmental pollution control, it is vital to develop a fast, simple, and sensitive method for analysis of OP pesticides in environmental samples.

Many analytical techniques, including capillary electrophoresis [6], gas or liquid chromatography [7–9] and electrochemical method [10,11], have been applied to develop sensitive, convenient and effective methods for OP pesticides residue analysis. Chromatography techniques operate with high sensitivity, accuracy and high throughput, instrumental analysis, but they suffer from complicated pretreatment steps using toxic organic solvent and also long analysis time, and most of them require expensive equipment [12]. Electrochemical method possesses high sensitivity, good selectivity and low-cost instrumentation. Electroanalysis can be used to give appropriate results within a short time under field conditions or on-line monitoring, which is very fit to analyze OP pesticides concentration in environmental samples.

Among the electrochemical methods, enzyme-based electrochemical biosensors have developed in the past few years to

* Corresponding author. Tel.: +86 21 62237105; fax: +86 21 62237105.
E-mail address: gyshi@chem.ecnu.edu.cn (G. Shi).

0304-3894/$ – see front matter © 2012 Elsevier B.V. All rights reserved.
doi:10.1016/j.jhazmat.2012.03.033

monitor OP pesticides [13–17]. However, the denaturation of enzymes results in the unstability and short lifetime of use for the sensor, which mostly limits the operational applications. In addition, the enzyme can be inhibited by many kinds of contamination such as heavy metals in environmental samples, which makes the direct determination of OP pesticides lack of selectivity and even leads to false positive result [18]. Therefore, in order to eliminate the influence of enzyme on the analysis of OP pesticides in environmental samples, some more effective methods were proposed to directly detect OP pesticides without using enzymes. Recently, electrochemical sensors based materials with no enzymes have been used in the fabrication of OP pesticides electrochemical sensors [10,11,19–29], such as ZrO_2 nanoparticles [10], nanometer-sized titania [11], Pd/MWCNTs nanocomposite [19], and pSC6 modified silver [23]. ZrO_2-nanoparticles modified electrode was fabricated for the detection of OP pesticides based on a strong affinity between nano-ZrO_2 and OP pesticides molecules [10,21,22,24]. Hu and co-workers developed a novel and simple sensor for dichlofenthion based on nanometer-sized titania photocatalysis coupled with a screen-printed carbon electrode [11]. Pd/MWCNTs nanocomposite modified electrode was developed for the determination of methyl parathion [19]. Li and co-workers presented pSC6 modified silver nanoparticles electrochemically deposited on glassy carbon electrode for electrochemical detection of methyl parathion [23].

Multiwalled carbon nanotubes (MWCNTs) as nanomaterial have attracted great attention for their unique structural, mechanical, and electrical properties since their discovery [30]. In order to introduce functional groups on MWCNTs and broaden the application fields of MWCNTs, composite materials based on the desirable merging of MWCNTs and polymers have gained growing interest [31,32]. Recent electrochemical studies reveal that the nanocomposite of MWCNTs and polymers are very promising in the design of electrochemical sensors and biosensors [31–36]. For example, MWCNTs and poly(methacrylic acid) (PMAA) nanocomposites prepared by free radical polymerization has been used for the detection of uric acid [32]. MWCNTs and polyaniline nanocomposites achieved by electrochemical grafting have been used for the determination of pesticides [33] and glucose [36]. In this work, a sensitive electrochemical differential pulse voltammetry method was developed for detecting methyl parathion (MP) based on MWCNTs–PAAM nanocomposite film modified glassy carbon electrode. The novel MWCNTs–PAAM nanocomposite, containing high content of amide groups, was synthesized by PAAM polymerizing at the vinyl group functionalized MWCNTs surface using free radical polymerization. The amino functionalized material exhibited good adsorption for OP pesticides molecules [37]. Similarly, the MWCNTs–PAAM/GCE showed a high adsorption and strong affinity toward MP compared with some metal ions and nitroaromatic compounds, which exist in environmental samples. The detection of MP for MWCNTs–PAAM/GCE was performed rapidly with wide linear range (5.0×10^{-9}–1.0×10^{-5} mol L^{-1}) and low detection limit of 2×10^{-9} mol L^{-1} (S/N = 3), which was better than some traditional materials modified electrode [1,10,19,20,23,25–29]. These merits made it suitable for MP determination in environmental water samples.

2. Experimental

2.1. Reagents

MWCNTs-COOH were obtained from Shenzhen Nanotech. Co., Ltd. (Shenzhen, China). Acrylamide (AAM), 2,4,6-trinitrotoluene (TNT), 2,4-dinitrotoluene (DNT), 1,3-dinitrobenzene (DNB) and ethylene glycol dimethacrylate (EGDMA) were purchased from Sigma–Aldrich Chemical Co. (USA). Methyl parathion (MP) was obtained from Dr. Ehrenstorfer GmbH Co. (Germany). 3-Aminopropyltriethoxysilane (APTES) and vinyltriethoxysilane (VTEOS) were purchased from TCI Co., Ltd. (Japan). Azodiisobutyronitrile (AIBN) was purchased from Sinopharm Group Chemical Regent Co., Ltd. (Shanghai, China). Other chemicals used were of analytical grade, and purchased from Sinopharm Group Chemical Regent Co., Ltd. (Shanghai, China). All compounds were used without further purification. The stock solution (0.001 mol L^{-1} MP) was prepared in ethanol and stored at 4 °C. Phosphate buffer solution (PBS, 0.2 M, pH 7.0) was prepared with NaH_2PO_4 and Na_2HPO_4. Double distilled water was used throughout.

2.2. Apparatus

Electrochemical measurements were performed on a CHI 660c electrochemical workstation (CH Instruments Co., Shanghai, China) with a conventional three electrode system comprising platinum wire as auxiliary electrode, saturated calomel electrode (SCE) as reference electrode and the modified or unmodified glass carbon electrode (3 mm diameter, GCE) as working electrode, containing a 10 mL of glass cell.

Fourier transform infrared spectroscopic measurements were performed on NEXUS 670 Fourier transform infrared spectrometer (Nicolet, USA). Thermal gravimetric analysis (TGA) was conducted on a TGA/SDTA851e instrument from room temperature to 600 °C with a heating rate of 10 °C min^{-1} in the nitrogen flow (Mettler Toledo Co., Switzerland). Surface morphological images were taken by a HITACHI S-4800 scanning electronic microscopy (Hitachi Co. Ltd., Tokyo, Japan).

2.3. Preparation of MWCNTs–PAAM nanocomposite

2.3.1. Synthesis of MWCNTs-COCl

A suspension of 0.3 g of MWCNTs-COOH in 30 mL of $SOCl_2$ was placed in a 100 mL round bottom flask and refluxed at 80 °C for 24 h under a dry air atmosphere [38]. The solid was washed by anhydrous tetrahydrofuran for several times to remove the excess $SOCl_2$ and dried in a vacuum oven to give MWCNTs-COCl.

2.3.2. Synthesis of MWCNTs–APTES

0.3 g MWCNTs-COCl obtained as outlined above was reacted with 25 mL of APTES in 25 mL of N-N′dimethyl formamide (DMF) under a dry air atmosphere at 120 °C for 48 h. 0.2 mL of triethylamine was added as phase transfer catalyst. After reaction, the product was filtered, washed with ethanol, and dried in a vacuum oven overnight, giving MWCNTs–$CONH(CH_2)_3Si(OC_2H_5)_3$ (MWCNTs–APTES).

2.3.3. Synthesis of MWCNTs—Si—C═C

The C═C modified MWCNTs was synthesized based on the reaction between MWCNTs–APTES and VTEOS with the method of aqueous ammonia as catalyst [39]. 1.0 mL of VTEOS was added to a suspension of 0.1 g MWCNTs–APTES in 20 mL of toluene. The above solution was stirred for 10 min, and then 0.5 mL of aqueous ammonia as catalyst was added. The mixture was stirred at room temperature over night. The product was collected by centrifugation and washed with ethanol. The solid was dried over night in a vacuum oven to obtain vinyl group functionalized MWCNTs (MWCNTs—Si—C═C).

2.3.4. Preparation of PAAM polymerizing on the surface of MWCNTs

40 mg of MWCNTs—Si—C═C was suspended in 20 mL of chloroform in a 100 mL round bottom flask. AAM (0.5 mmol) and EGDMA (2.5 mmol) were added into the above solution and stirred for 1 h. Then, 10 mg of AIBN as the initiator was added and the mixture

was purged with nitrogen to remove oxygen for 15 min. Finally, the polymerizing reaction was allowed to process at 60 °C for 24 h. The resulting product was collected by centrifugation and was washed by ethanol to remove the unreacted AAM, EGDMA and initiator. Then the solid was dried overnight in a vacuum oven to obtain MWCNTs–PAAM nanocomposite. For comparison, PAAM was prepared by the same procedure, only without using MWCNTs—Si—C=C in the polymerization process.

2.4. Preparation of MWCNTs–PAAM modified GCE

Prior to the modification, glassy carbon electrode (GCE) was polished with alumina slurry, then it was washed in an ultrasonic bath first with nitric acid solution (1:1, v/v), then with ethanol and finally with water (3 min each). 2 mg of MWCNTs–PAAM nanocomposite was dispersed in 1 mL of DMF with ultrasonic for 30 min. The above suspension (4 μL) was dropped on the clean GCE surface, and the solvent was evaporated under an infrared lamp. Thus, the MWCNTs–PAAM/GCE was obtained. The PAAM/GCE was prepared under the same conditions.

2.5. Electrochemical experiments

PBS buffer (0.2 M, pH 7.0) solution was used as the supporting electrolyte. The electrolyte solution was purged with nitrogen for 10 min and maintained under nitrogen atmosphere during the measurements. As shown in Scheme 1, the modified electrode was dipped into the desired concentration of MP in double distilled water for 5 min, and washed with double distilled water to remove the possible adsorptive substances on the electrode surface. Then, differential pulse voltammograms of the modified electrode which had absorbed MP were recorded between −0.3 and −1.0 V. The pulse amplitude, pulse period, and pulse width of DPV were 50 mV, 0.2 s, and 50 ms, respectively. The cathodic peak current was measured at −0.72 V. Cyclic voltammetry was performed from 0.4 to −1.0 V under similar conditions.

3. Results and discussion

3.1. Preparation and characterization of MWCNTs–PAAM nanocomposite

The preparation of MWCNTs–PAAM nanocomposite was illustrated in Scheme 1. Details of the preparation could be found in Section 2. The MWCNTs–PAAM nanocomposite was characterized by Fourier transform infrared spectroscopy (FT-IR spectroscopy), thermal gravimetric analysis (TGA) and scanning electron microscopy (SEM).

3.1.1. FT-IR spectroscopy analysis

FT-IR spectroscopy was employed to characterize the MWCNTs-COOH, MWCNTs—Si—CH=CH_2 and MWCNTs–PAAM nanocomposite and the spectrograms were shown in Fig. 1. It can be seen from Fig. 1a that the absorption band of MWCNTs-COOH situating around 3436 cm^{-1} was assigned to O—H stretching of carboxylic group. In Fig. 1b, a peak at 3055 cm^{-1} was assigned to C—H stretching vibration, which belonged to the group of —HC=CH_2. The absorbance at 1630 cm^{-1} and 1579 cm^{-1} were assigned to C=O and C=C stretch vibration, respectively. The bands around 1047 cm^{-1} and 765 cm^{-1} resulted from Si—O vibrations. The results indicated that VTEOS was successfully grafted on the MWCNTs. As shown in Fig. 1c, the strong bands around 3600–3300 cm^{-1} resulted from O—H and N—H stretching vibrations, indicating the MWCNTs–PAAM nanocomposite had high amide content. The absorption bands of MWCNTs–PAAM nanocomposite situating around 1726 cm^{-1} and 1454 cm^{-1} were assigned to the following vibrations: C=O and C—N stretching vibrations, respectively. All these absorption bands suggested the successful synthesis of MWCNTs–PAAM nanocomposite.

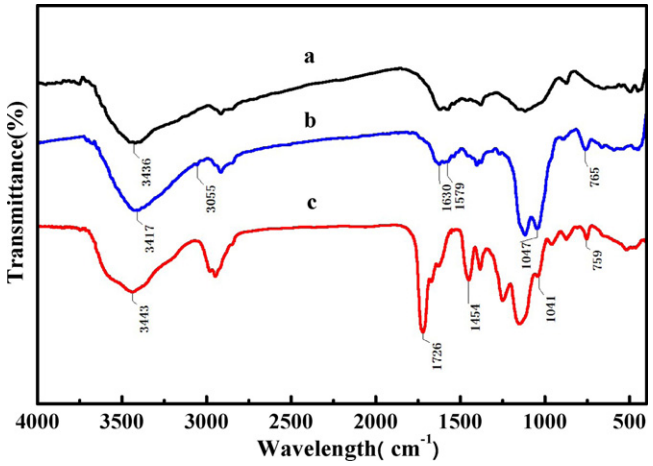

Fig. 1. FT-IR spectra of MWCNTs-COOH (a), MWCNTs—Si—CH=CH_2 (b), MWCNTs–PAAM nanocomposite (c).

3.1.2. TGA characterization

On the basis of the different thermal stability between the polymers and MWCNTs, the TGA measurements were used to provide evidence regarding the content of grafted PAAM on the surface of MWCNTs. Fig. 2 showed TGA weight loss curves of MWCNTs-COOH, MWCNTs–PAAM nanocomposite and PAAM, respectively. As shown in Fig. 2a, the MWCNTs-COOH was steady with a little weight loss below 600 °C. However, the TGA curve of PAAM showed a gradual weight loss below 300 °C, which was likely due to the decomposition of labile oxygen functional groups (Fig. 2c). The weight of PAAM declined sharply between 300 °C and 400 °C, which might be corresponding to the degradation of carbon skeleton. The whole weight was almost lost at 430 °C. Analogously, the MWCNTs–PAAM nanocomposite also appeared to have a similar weight loss trend with the temperature increasing, and it became stable above 450 °C with about 90% total weight loss (Fig. 2b). The difference in the weight loss between PAAM and MWCNTs–PAAM nanocomposite (total weight loss and 90% total weight loss) revealed that PAAM were successfully grafted on the MWCNTs surface.

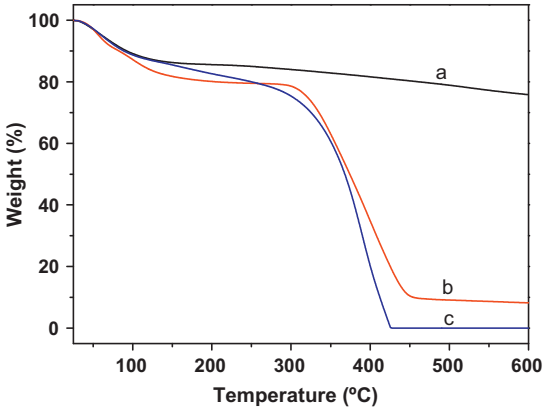

Fig. 2. TGA weight loss curves of MWCNTs-COOH (a), MWCNTs–PAAM nanocomposite (b) and PAAM (c).

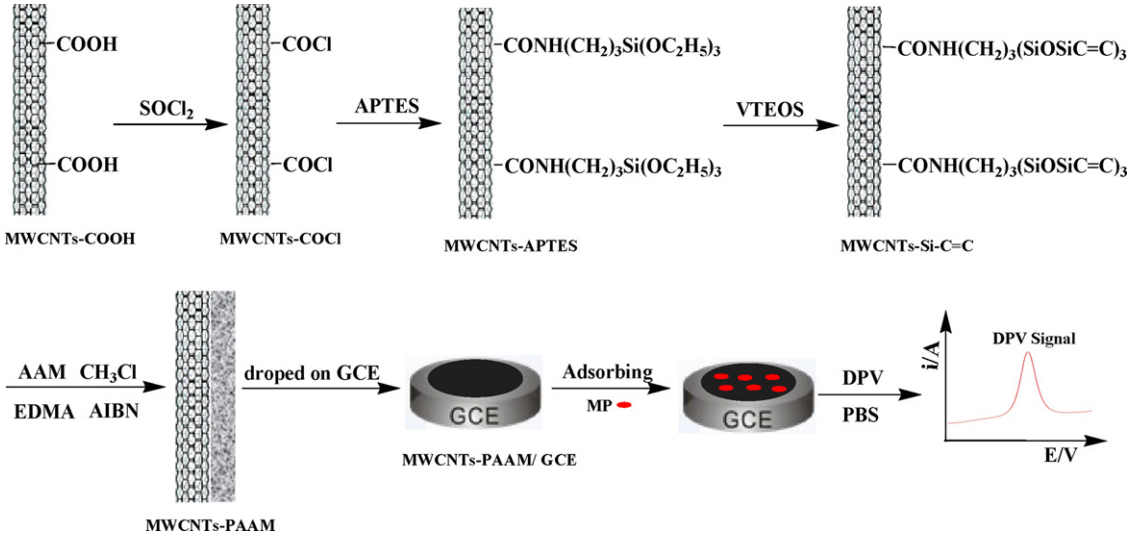

Scheme 1. The preparation steps for the MWCNTs–PAAM nanocomposite, MWCNTs–PAAM/GCE and the process of electrochemical detecting method for MP.

3.1.3. Morphological characterization

SEM was used to characterize the morphologies of the crude MWCNTs-COOH, MWCNTs—Si—C=C, MWCNTs–PAAM nanocomposite and PAAM. The average thickness of the MWCNTs-COOH was about 20 nm (Fig. 3a). The SEM of MWCNTs—Si—C=C was similar to that of MWCNTs-COOH (Fig. 3b). After the polymerization, the MWCNTs were coated with homogeneous polymers layer (Fig. 3c). The average size increased to 35 nm. Thus, it was calculated that the average thickness of the PAAM polymers layer on the surface of MWCNTs was about 15 nm. For comparison, it can be seen from Fig. 3d that the PAAM had a porous structure nanomaterial. In addition, from the porous nanostructure of PAAM on the MWCNTs, it could be deduced that the surface structure of MWCNTs–PAAM nanocomposite was porous.

3.2. Electrochemical behavior of MP on the MWCNTs–PAAM/GCE

The preparation of MWCNTs–PAAM/GCE and electrochemical experiments was performed according to Scheme 1 and Sections 2.4 and 2.5. The cyclic voltammograms (CV) of MWCNTs–PAAM/GCE in the absence (a) and presence (b and c) of 5.0×10^{-6} mol L^{-1} MP were shown in Fig. 4(A). There was no redox peak of CV observed at the MWCNTs–PAAM/GCE in 0.2 M PBS blank solution. However, MP exhibited well-defined voltammetric peaks,

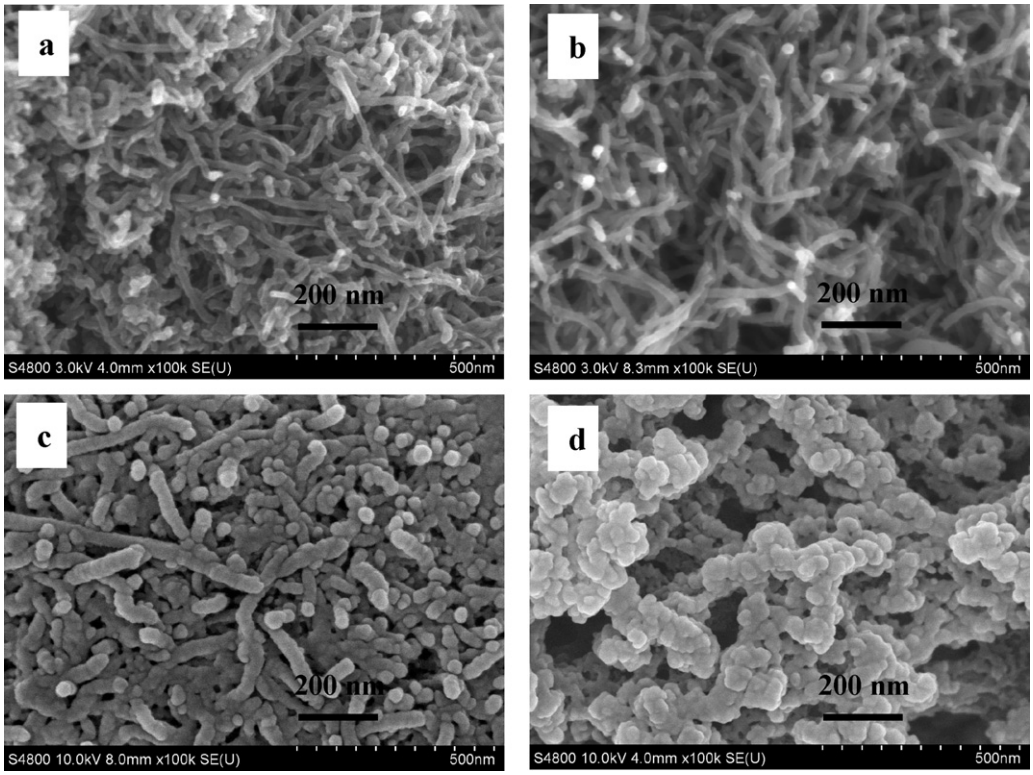

Fig. 3. SEM images of MWCNTs-COOH (a); MWCNTs—Si—CH=CH_2 (b); MWCNTs–PAAM nanocomposite (c); PAAM (d).

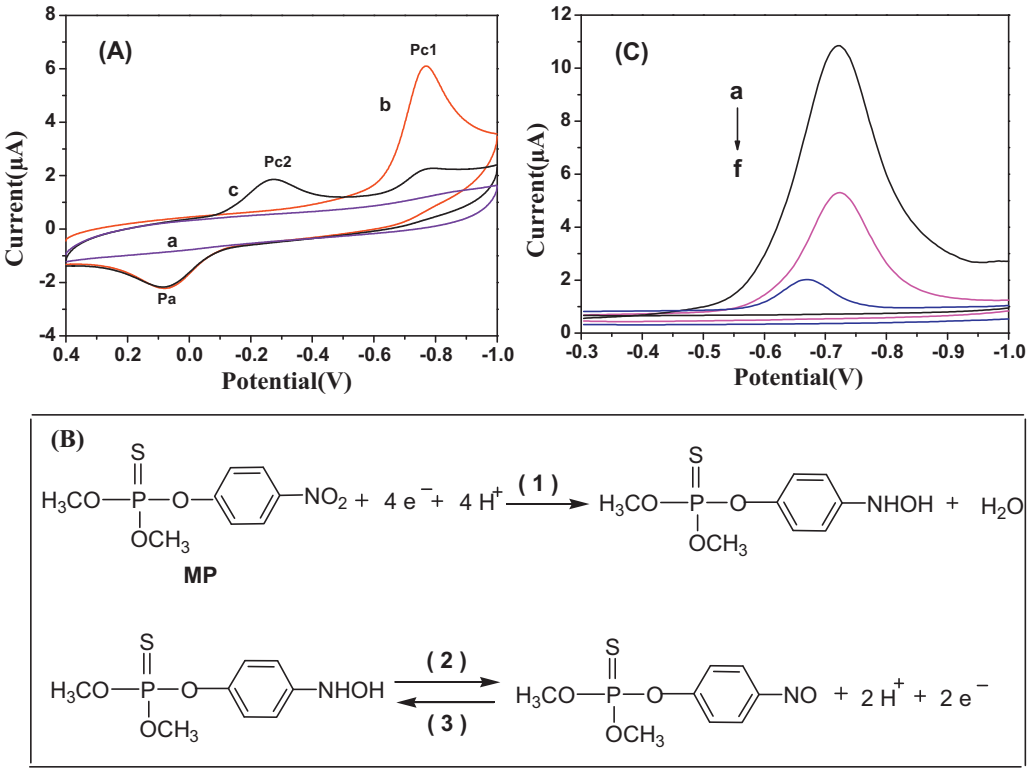

Fig. 4. (A) CV of MWCNTs–PAAM/GCE in the absence (a) and presence (b and c) of 5.0×10^{-6} mol L^{-1} MP; (B) mechanism of the electrochemical reaction of MP at MWCNTs–PAAM/GCE; (C) DPV of MWCNTs–PAAM/GCE (a and d), PAAM/GCE (b and e) and GCE (c and f) in the presence (a, b and c) and absence (d, e and f) of 1.0×10^{-5} mol L^{-1} MP; supporting electrolyte, 0.2 M PBS (pH 7.0); scan rate, 100 mV s^{-1}; adsorption time, 5 min.

which were observed at the MWCNTs–PAAM/GCE in presence of 5.0×10^{-6} mol L^{-1} MP. In the first cycle (Fig. 4(A), curve b), a sharp irreversible reduction peak (E_{pc1}, −0.769 V) can be observed, which corresponded to the reduction of the nitro group to hydroxylamine group via a four-electron process [40] (reaction 1, Fig. 4(B)). Then it was oxidized to the nitroso group (E_{pa}, 0.078 V, reaction 2). In the following second cycle (Fig. 4(A), curve c), the appearance of another reduction peak (E_{pc2}, −0.274 V, reaction 3) was ascribed to reverse process of reaction 2. The pair of reversible redox peaks should be attributed to a two-electron transfer redox process. The peak Pc1 reduced in the second cycle, which should be due to the reaction exhaustion of methyl parathion at the surface of MWCNTs–PAAM/GCE.

It was shown in Fig. 4(C) that differential pulse voltammograms (DPV) of MWCNTs–PAAM/GCE (a and d), PAAM/GCE (b and e) and GCE (c and f) in the presence (a, b and c) and absence (d, e and f) of MP were recorded between −0.3 and −1.0 V. There was no redox peak of DPV observed at the MWCNTs–PAAM/GCE, PAAM/GCE and GCE in 0.2 M PBS blank solution. However, the well-defined peaks, which should be attributed to the irreversible reduction of the nitro group to hydroxylamine group, were observed at −0.72 V of MP for MWCNTs–PAAM/GCE and PAAM/GCE. The peak current of MP measured by DPV at MWCNTs–PAAM/GCE was higher than that at PAAM/GCE and bare GCE, which suggested that MWCNTs–PAAM/GCE could display better electrochemical activities toward MP compared with PAAM/GCE and bare GCE. The experimental results revealed that MWCNTs–PAAM/GCE possessed better catalytic activity toward the electroreduction of MP, which could be attributed to the synthesized MWCNTs–PAAM nanocomposite based on MWCNTs matrix [33–36]. In addition, the phenomenon for current enhancement can be explained from the larger electrochemical effective surface area of MWCNTs–PAAM/GCE [41,42].

3.3. Electrochemical effective surface area

The electrochemical effective surface area for MWCNTs–PAAM/GCE, PAAM/GCE and bare GCE can be calculated by the slope of the plot of Q vs. $t^{1/2}$ obtained by chronocoulometry using 0.25 mM $K_3[Fe(CN)_6]$ as model complex based on Eq. (1) given by Anson [43]:

$$Q(t) = \frac{2nFACD^{1/2}t^{1/2}}{\pi^{1/2}} + Q_{dl} + Q_{ads} \quad (1)$$

where A is the surface area of the working electrode, c is the concentration of substrate, D is the diffusion coefficient (D of $K_3[Fe(CN)_6]$ is 7.6×10^{-6} cm^2 s^{-1} [44]), Q_{dl} is double layer charge which could be eliminated by background subtraction, Q_{ads} is Faradic charge. As showed in Fig. 5, the slope of the linear relationship between Q and $t^{1/2}$ for MWCNTs–PAAM/GCE, PAAM/GCE and bare GCE can be obtained to be 1.1×10^{-5}, 7.64×10^{-6} and 5.0×10^{-6}, respectively. Thus, A can be calculated to be 0.146 cm^2, 0.102 cm^2 and 0.067 cm^2 for MWCNTs–PAAM/GCE, PAAM/GCE and bare GCE, respectively. The results indicated that the electrochemical effective surface area was increased obviously after modification of GCE with MWCNTs–PAAM, which could enhance the total adsorption capacity of MP, leading to the increase of current response of MP [42], decreasing the limit of detection.

3.4. Influence of adsorption time on the response of MP

The influence of adsorption time on the response of MP at MWCNTs–PAAM/GCE was investigated in Fig. 6. The MWCNTs–PAAM/GCE was dipped into 3.0×10^{-6} mol L^{-1} MP solution under different adsorption times. According to Fig. 6, the DPV peak current increased rapidly with 3 min of adsorption time. Then, the adsorption amount of MP would reach saturation after 5 min

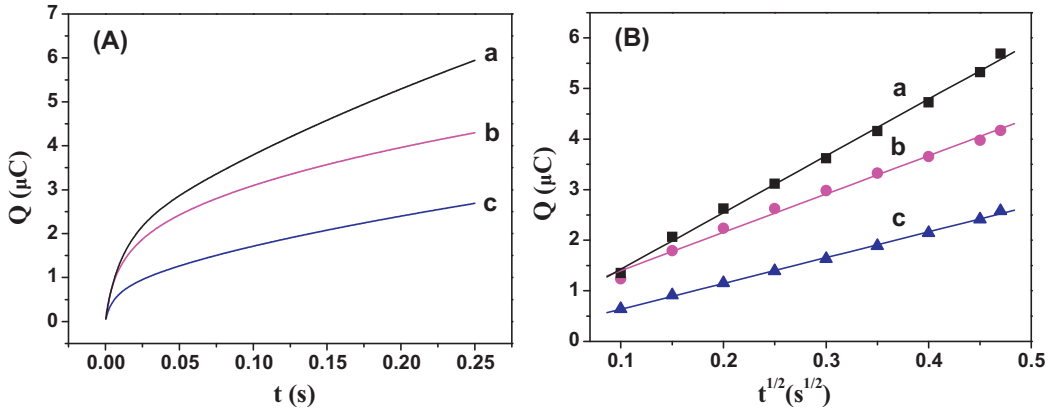

Fig. 5. (A): Plot of Q–t curves for the MWCNTs–PAAM/GCE (a), PAAM/GCE (b) and GCE (c) in 0.25 mM $K_3[Fe(CN)_6]$; (B): plot of Q–$t^{1/2}$ curves for the MWCNTs–PAAM/GCE (a), PAAM/GCE (b) and GCE (c) in 0.25 mM $K_3[Fe(CN)_6]$. The pulse width, sample interval and quiet time of chronocoulometry were 0.25 s, 0.25 ms, and 2 s, respectively.

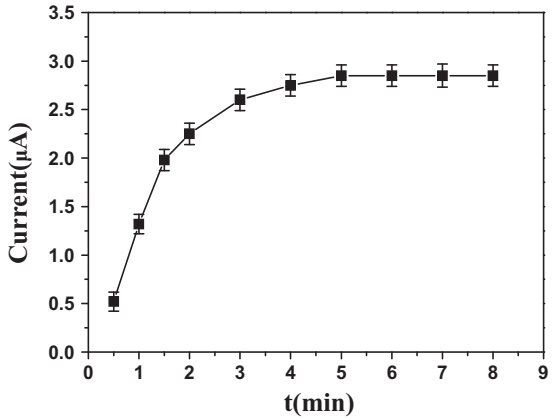

Fig. 6. The influence of adsorption time on the DPV response of MP at MWCNTs–PAAM/GCE, MP concentration: 3.0×10^{-6} mol L^{-1}; supporting electrolyte, 0.2 M PBS (pH 7.0); scan rate, 100 mV s^{-1}.

of adsorption time. Thus, 5 min of adsorption time was employed. Form the experiments of electrochemical effective surface area and adsorption time for MWCNTs–PAAM/GCE, it can be seen that MWCNTs–PAAM nanocomposite should have good adsorption capacity for MP, which could be attributed to the interaction between MP and the amino group of MWCNTs–PAAM nanocomposite [37,45].

3.5. Linearity, stability and reproducibility of sensor

The analytical features of linearity, stability and reproducibility were investigated. As can be seen from Fig. 7, the peak current linearly increased with the MP concentration in the range of 5.0×10^{-9}–1.0×10^{-5} mol L^{-1}. The linear equation was i_{pc} (μA) = 0.1988 + 0.8819C (μM) (R^2 = 0.9987). The detection limit of MP determination for MWCNTs–PAAM/GCE was found to be 2.0×10^{-9} mol L^{-1} (S/N = 3), which was better than some traditional materials modified electrode (Table 1) [1,10,19,20,23,25–29]. Moreover, the sensitivity of MWCNTs–PAAM/GCE was 0.882 μA [μM]$^{-1}$, which was higher than some of the modified electrode, such as surfactant–clay/GCE [1], ZrO_2/CPE [10], Au–nafion/GCE [20] and Au/MWCNTs electrode [29].

The reproducibility and stability of MWCNTs–PAAM/GCE were investigated by the determination of 3.0×10^{-6} mol L^{-1} MP. DPV experiments were repeatedly performed for 8 times with the same modified electrode in the solution of 3.0×10^{-6} mol L^{-1} MP. The relative standard deviation was 4.3%. Similarly, the fabrication reproducibility was estimated by using eight different electrodes. A solution containing 3.0×10^{-6} mol L^{-1} MP was determined by eight electrodes in the same electrochemical cell, with a relative standard deviation of 4.5%. It indicated the good reproducibility of the modified electrode. The stability of the MWCNTs–PAAM/GCE was also examined in this work. A response of 93.6% of the initial current was retained for the electrode after it was stored in refrigerator for two weeks.

Table 1
The comparison of the proposed method with other reported methods of MP determination.

Detection methods	Linear range (mol L^{-1})	Detection limit (mol L^{-1})	Sensitivity (μA [μM]$^{-1}$)	References
Surfactant–clay/GCE	4.0×10^{-7}–8.5×10^{-6}	7.0×10^{-8}	0.576	[1]
ZrO_2/CPE[a]	1.9×10^{-8}–1.1×10^{-5}	7.6×10^{-9}	0.359	[10]
Pd/MWCNTs/GCE	3.8×10^{-7}–5.3×10^{-5}	1.9×10^{-7}	4.82	[19]
Au–nafion/GCE	5.0×10^{-7}–1.2×10^{-4}	1.0×10^{-7}	0.257	[20]
pSC6–AgNPs[b]/GCE	1.0×10^{-8}–8.0×10^{-5}	4.0×10^{-9}	11.6	[23]
OMC[c]/GCE	9.0×10^{-8}–6.1×10^{-5}	7.6×10^{-9}	1.31	[25]
Silicate–CTAB[d]/GCE	1.0×10^{-7}–1.0×10^{-4}	1.0×10^{-8}	1.01	[26]
C/p-NiTSPc[e]/CFME[f]	3.8×10^{-8}–3.8×10^{-5}	1.5×10^{-7}	0.021	[27]
MWCNTs–chitosan/GCE	1.9×10^{-7}–7.6×10^{-6}	1.9×10^{-8}	Not reported	[28]
Au/MWCNTs electrode	1.9×10^{-6}–6.1×10^{-5}	1.9×10^{-7}	0.503	[29]
MWCNTs–PAAM/GCE	5.0×10^{-9}–1.0×10^{-5}	2.0×10^{-9}	0.882	This work

[a] CPE: carbon paste electrode.
[b] pSC6–AgNPs: para-sulfonatocalix[6]arene-modified silver nanoparticles.
[c] OMC: ordered mesoporous carbon.
[d] CTAB: cetyltrimethylammonium bromide.
[e] C/p-NiTSPc: tetrasulfonated nickel phtalocyanine.
[f] CFME: coated carbon fiber microelectrode.

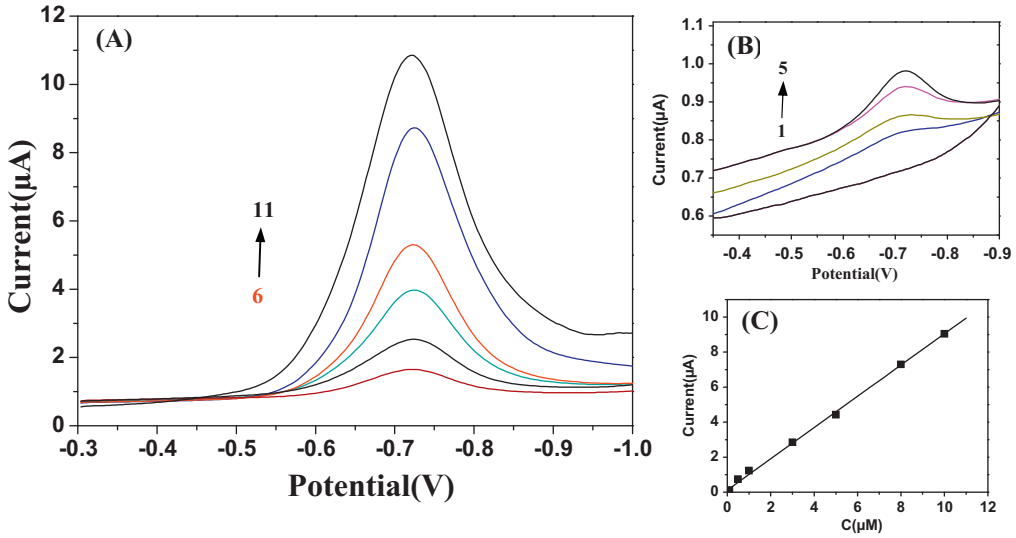

Fig. 7. (A) DPV for MP at MWCNTs–PAAM/GCE. MP concentration (1–11):0, 5.0×10^{-9}, 1.0×10^{-8}, 5.0×10^{-8}, 1.0×10^{-7}, 5.0×10^{-7}, 1.0×10^{-6}, 3.0×10^{-6}, 5.0×10^{-6}, 8.0×10^{-6}, 1.0×10^{-5} mol L^{-1}. (B) DPV for MP at MWCNTs–PAAM/GCE. MP concentration (1–5): 0, 5.0×10^{-9}, 1.0×10^{-8}, 5.0×10^{-8}, 1.0×10^{-7} mol L^{-1}. (C) The calibration curve for the proposed method. Supporting electrolyte, 0.2 M PBS (pH 7.0); scan rate, 100 mV s^{-1}; adsorption time, 5 min.

3.6. Interference studies

In order to apply the proposed method in environmental samples, it was vital to investigate the effect of some of the interfering ions and nitroaromatic compounds on MP, which was used to evaluate the selectivity of the MWCNTs–PAAM/GCE to MP. The DPV determination of MP was tested in the presence of spiked known amounts of interfering ions and nitroaromatic compounds. The tolerance limit was defined as the amount and fold of the interfering substances causing a change of ±5% in the peak current intensity reading. The tolerable limits of interfering substances were given in Table 2. The results indicated that the MWCNTs–PAAM/GCE exhibited a high adsorption and strong affinity toward MP compared with some metal ions and nitroaromatic compounds, which exist in environmental water samples.

3.7. Analytical application

To demonstrate the feasibility of the MWCNTs–PAAM/GCE, the proposed procedure was applied to the determination of MP in water samples collected from Tap water and Liwa river of East China Normal University. The real water samples were filtered with a 0.45 μm filter to eliminate particulate matters. The concentration values of MP in the water samples were determined by the proposed method. No voltammetric response corresponding to MP was observed when the real water samples were analyzed, thus different quantity of MP was added to the samples, respectively. Spiking method was adopted to evaluate the MP content of different samples. The results were summarized in Table 3. As can be seen from Table 3, the recoveries were from 96.4% to 101.8%. Thus, the proposed DPV procedure based on MWCNTs–PAAM/GCE can be applied for detecting MP in environmental water samples with good results.

Table 2
The tolerance limit of interfering substances on DPV determination of MP using the MWCNTs–PAAM/GCE. (Conditions: MP concentration, 3.0×10^{-6} mol L^{-1}; supporting electrolyte, 0.2 M PBS (pH 7.0); scan rate, 100 mV s^{-1}; adsorption time, 5 min).

Interfering substances	Tolerance limit (mol L^{-1}, fold)
Na^+, K^+, Cl^-, NO_3^-, SO_4^{2-}, CO_3^{2-}, PO_4^{3-}	6.0×10^{-3}, 2000
Ca^{2+}, Mg^{2+}, Zn^{2+}, Co^{2+}, Fe^{3+}	3.0×10^{-3}, 1000
Ni^{2+}, Cu^{2+}, Pb^{2+}	1.5×10^{-3}, 500
Fe^{2+}	6.0×10^{-4}, 200
para-Aminophenol	1.5×10^{-4}, 50
para-Nitrophenol	9.0×10^{-5}, 30
Nitrobenzene	3.0×10^{-5}, 10
DNB	1.5×10^{-5}, 5
TNT, DNT	6.0×10^{-6}, 2

Table 3
Determination of MP and recovery test of MP in tap and river water samples with the proposed method ($n = 6$). (Conditions: supporting electrolyte, 0.2 M PBS (pH 7.0); scan rate, 100 mV s^{-1}; adsorption time, 5 min).

Sample	Added MP (mol L^{-1})	Found MP (mol L^{-1})	Recovery (%)	RSD (%)
Tap water	2.0×10^{-7}	2.012×10^{-7}	100.6	4.3
Tap water	6.0×10^{-7}	5.892×10^{-7}	98.2	3.9
Tap water	1.0×10^{-6}	9.73×10^{-7}	97.3	3.2
River water	2.0×10^{-7}	2.036×10^{-7}	101.8	4.8
River water	6.0×10^{-7}	6.048×10^{-7}	100.8	4.5
River water	1.0×10^{-6}	9.64×10^{-7}	96.4	3.6

4. Conclusion

A sensitive and selective electrochemical differential pulse voltammetry method was developed for detecting MP based on MWCNTs–PAAM nanocomposite film modified glassy carbon electrode. The experimental results demonstrated that the MWCNTs–PAAM/GCE exhibited a high adsorption and strong affinity toward MP compared with some metal ions and nitroaromatic compounds. This MWCNTs–PAAM nanocomposite film electrode was proved to be a suitable sensing tool for the fast, sensitive and selective determination of MP in environmental water samples.

Acknowledgments

This work is supported by the National Natural Science Foundation of China (21175044). This work is also supported by the Programs of the Science & Technology Commission of Shanghai Municipality (10JC1404000) and the Natural Science Foundation of Shanghai (11ZR1410700). We also greatly thank the Research Fund for the Doctoral Program of Higher Education (20100076110002).

References

[1] H.L. Tcheumi, I.K. Tonle, E. Ngameni, A. Walcarius, Electrochemical analysis of methylparathion pesticide by a gemini surfactant-intercalated clay-modified electrode, Talanta 81 (2010) 972–979.

[2] M. Tankiewicz, J. Fenik, M. Biziuk, Determination of organophosphorus and organonitrogen pesticides in water samples, TrAC, Trends Anal. Chem. 29 (2010) 1050–1063.

[3] G. Lagaly, Pesticide–clay interactions and formulations, Appl. Clay. Sci. 18 (2001) 205–209.

[4] M.A. Islam, V. Sakkas, T.A. Albanis, Application of statistical design of experiment with desirability function for the removal of organophosphorus pesticide from aqueous solution by low-cost material, J. Hazard. Mater. 170 (2009) 230–238.

[5] J.J. Yang, C. Yang, H. Jiang, C.L. Qiao, Overexpression of methyl parathion hydrolase and its application in detoxification of organophosphates, Biodegradation 19 (2008) 831–839.

[6] M. Lecoeur-Lorin, R. Delepee, P. Morin, Simultaneous enantioselective determination of fenamiphos and its two metabolites in soil sample by CE, Electrophoresis 30 (2009) 2931–2939.

[7] T. Hyotylainen, K. Luthje, M. Rautiainen-Rama, M.L. Riekkola, Determination of pesticides in red wines with on-line coupled microporous membrane liquid–liquid extraction–gas chromatography, J. Chromatogr. A 1056 (2004) 267–271.

[8] S. Moinfar, M.R.M. Hosseini, Development of dispersive liquid–liquid microextraction method for the analysis of organophosphorus pesticides in tea, J. Hazard. Mater. 169 (2009) 907–911.

[9] J. Hassan, A. Farahani, M. Shamsipur, F. Damerchili, Rapid and simple low density miniaturized homogeneous liquid–liquid extraction and gas chromatography/mass spectrometric determination of pesticide residues in sediment, J. Hazard. Mater. 184 (2010) 869–871.

[10] H. Parham, N. Rahbar, Square wave voltammetric determination of methyl parathion using ZrO_2-nanoparticles modified carbon paste electrode, J. Hazard. Mater. 177 (2010) 1077–1084.

[11] H.B. Li, J. Li, Z.J. Yang, Q. Xu, X.Y. Hu, A novel photoelectrochemical sensor for the organophosphorus pesticide dichlofenthion based on nanometer-sized titania coupled with a screen-printed electrode, Anal. Chem. 83 (2011) 5290–5295.

[12] M. Sbai, H. Essis-Tome, U. Gombert, T. Breton, M. Pontie, Electrochemical stripping analysis of methyl-parathion (MPT) using carbon fiber microelectrodes (CFME) modified with combinations of poly-NiTSPc and Nafion® films, Sens. Actuators B 124 (2007) 368–375.

[13] F.N. Kok, V. Hasirci, Determination of binary pesticide mixtures by an acetylcholinesterase-choline oxidase biosensor, Biosens. Bioelectron. 19 (2004) 661–665.

[14] R.P. Deo, J. Wang, I. Block, A. Mulchandani, K.A. Joshi, M. Trojanowicz, F. Scholz, W. Chen, Y.H. Lin, Determination of organophosphate pesticides at a carbon nanotube/organophosphorus hydrolase electrochemical biosensor, Anal. Chim. Acta 530 (2005) 185–189.

[15] G.D. Liu, Y.H. Lin, Biosensor based on self-assembling acetylcholinesterase on carbon nanotubes for flow injection/amperometric detection of organophosphate pesticides and nerve agents, Anal. Chem. 78 (2006) 835–843.

[16] D. Du, W.J. Chen, W.Y. Zhang, D.L. Liu, H.B. Li, Y.H. Lin, Covalent coupling of organophosphorus hydrolase loaded quantum dots to carbon nanotube/Au nanocomposite for enhanced detection of methyl parathion, Biosens. Bioelectron. 25 (2010) 1370–1375.

[17] J.M. Gong, L.Y. Wang, L.Z. Zhang, Electrochemical biosensing of methyl parathion pesticide based on acetylcholinesterase immobilized onto Au-polypyrrole interlaced network-like nanocomposite, Biosens. Bioelectron. 24 (2009) 2285–2288.

[18] J.H. Zhou, C.Y. Deng, S.H. Si, S.E. Wang, Zirconia electrodeposited on a self-assembled monolayer on a gold electrode for sensitive determination of parathion, Microchim. Acta 172 (2011) 207–215.

[19] B. Huang, W.D. Zhang, C.H. Chen, Y.X. Yu, Electrochemical determination of methyl parathion at a Pd/MWCNTs-modified electrode, Microchim. Acta 171 (2010) 57–62.

[20] T.F. Kang, F. Wang, L.P. Lu, Y. Zhang, T.S. Liu, Methyl parathion sensors based on gold nanoparticles and Nafion film modified glassy carbon electrodes, Sens. Actuators B 145 (2010) 104–109.

[21] M. Wang, Z.Y. Li, Nano-composite ZrO_2/Au film electrode for voltammetric detection of parathion, Sens. Actuators B 133 (2008) 607–612.

[22] J.H. Zhou, C.Y. Deng, S.H. Si, S.E. Wang, Zirconia electrodeposited on a self-assembled monolayer on a gold electrode for sensitive determination of parathion, Microchim. Acta 172 (2010) 207–215.

[23] Y.H. Bian, C.Y. Li, H.B. Li, para-Sulfonatocalix[6] arene-modified silver nanoparticles electrodeposited on glassy carbon electrode: preparation and electrochemical sensing of methyl parathion, Talanta 81 (2010) 1028–1033.

[24] D. Du, X.P. Ye, J.D. Zhang, Y. Zeng, H.Y. Tu, A.D. Zhang, D.L. Liu, Stripping voltammetric analysis of organophosphate pesticides based on solid-phase extraction at zirconia nanoparticles modified electrode, Electrochem. Commun. 10 (2008) 686–690.

[25] D. Pan, S.M. Ma, X.J. Bo, L.P. Guo, Electrochemical behavior of methyl parathion and its sensitive determination at a glassy carbon electrode modified with ordered mesoporous carbon, Microchim. Acta 173 (2011) 215–221.

[26] S.C. Xia, J.F. Zhang, C.Y. Li, Electrochemical deposition of silicate-cetyltrimethylammonium bromide nanocomposite film on glassy carbon electrode for sensing of methyl parathion, Anal. Bioanal. Chem. 396 (2009) 697–705.

[27] I. Tapsoba, S. Bourhis, T. Feng, M. Pontié, Sensitive and selective electrochemical analysis of methyl-parathion (MPT) and 4-nitrophenol (PNP) by a new type p-NiTSPc/p-PPD coated carbon fiber microelectrode (CFME), Electroanalysis 21 (2009) 1167–1176.

[28] D. Du, M.H. Wang, J.M. Zhang, J. Cai, H.Y. Tu, A.D. Zhang, Application of multiwalled carbon nanotubes for solid-phase extraction of organophosphate pesticide, Electrochem. Commun. 10 (2008) 85–89.

[29] J.C. Ma, W.D. Zhang, Gold nanoparticle-coated multiwall carbon nanotube-modified electrode for electrochemical determination of methyl parathion, Microchim. Acta 175 (2011) 309–314.

[30] S. Iijima, Helical microtubules of graphitic carbon, Nature 354 (1991) 56–58.

[31] Z. Spitalsky, D. Tasis, K. Papagelis, C. Galiotis, Carbon nanotube–polymer composites: chemistry, processing, mechanical and electrical properties, Prog. Polym. Sci. 35 (2010) 357–401.

[32] P.Y. Chen, P.C. Nien, C.W. Hu, K.C. Ho, Detection of uric acid based on multi-walled carbon nanotubes polymerized with a layer of molecularly imprinted PMAA, Sens. Actuators B 146 (2010) 466–471.

[33] P. Manisankar, P.L.A. Sundari, R. Sasikumar, S.P. Palaniappan, Electroanalysis of some common pesticides using conducting polymer/multiwalled carbon nanotubes modified glassy carbon electrode, Talanta 76 (2008) 1022–1028.

[34] C. Dhand, S.K. Arya, M. Datta, B.D. Malhotra, Polyaniline–carbon nanotube composite film for cholesterol biosensor, Anal. Biochem. 383 (2008) 194–199.

[35] Y. Li, Y. Umasankar, S.M. Chen, Polyaniline and poly(flavin adenine dinucleotide) doped multi-walled carbon nanotubes for p-acetamidophenol sensor, Talanta 79 (2009) 486–492.

[36] H.A. Zhong, R. Yuan, Y.Q. Chai, W.J. Li, X. Zhong, Y. Zhang, In situ chemosynthesized multi-wall carbon nanotube–conductive polyaniline nanocomposites: characterization and application for a glucose amperometric biosensor, Talanta 85 (2011) 104–111.

[37] H. Bagheri, Z. Ayazi, E. Babanezhad, A sol–gel-based amino functionalized fiber for immersed solid-phase microextraction of organophosphorus pesticides from environmental samples, Microchem. J. 94 (2010) 1–6.

[38] C. Zheng, M. Feng, Y.H. Du, H.B. Zhan, Synthesis and third-order nonlinear optical properties of a multiwalled carbon nanotube–organically modified silicate nanohybrid gel glass, Carbon 47 (2009) 2889–2897.

[39] W.H. Zhao, N. Sheng, R. Zhu, F.D. Wei, Z. Cai, M.J. Zhai, S.H. Du, Q. Hu, Preparation of dummy template imprinted polymers at surface of silica microparticles for the selective extraction of trace bisphenol A from water samples, J. Hazard. Mater. 179 (2010) 223–229.

[40] G.D. Liu, Y.H. Lin, Electrochemical sensor for organophosphate pesticides and nerve agents using zirconia nanoparticles as selective sorbents, Anal. Chem. 77 (2005) 5894–5901.

[41] J.H. Li, D.Z. Kuang, Y.L. Feng, F.X. Zhang, Z.F. Xu, M.Q. Liu, A graphene oxide-based electrochemical sensor for sensitive determination of 4-nitrophenol, J. Hazard. Mater. 201–202 (2012) 250–259.

[42] H.S. Yin, L. Cui, S.Y. Ai, H. Fan, L.S. Zhu, Electrochemical determination of bisphenol A at Mg–Al–CO_3 layered double hydroxide modified glassy carbon electrode, Electrochim. Acta 55 (2010) 603–610.

[43] F. Anson, Application of potentiostatic current integration to the study of the adsorption of cobalt (III)–(ethylenedinitrilo (tetraacetate)) on mercury electrodes, Anal. Chem. 36 (1964) 932–934.

[44] R. Adams, Electrochemistry at Solid Electrodes, M. Dekker, New York, 1969.

[45] C.G. Xie, H.F. Li, S.Q. Li, J. Wu, Z.P. Zhang, Surface molecular self-assembly for organophosphate pesticide imprinting in electropolymerized poly(p-aminothiophenol) membranes on a gold nanoparticle modified glassy carbon electrode, Anal. Chem. 82 (2010) 241–249.